[CANCER RESEARCH 64, 6327–6336, September 1, 2004]

Bone Marrow Stroma Influences Transforming Growth Factor-β Production in Breast Cancer Cells to Regulate c-myc Activation of the Preprotachykinin-I Gene in Breast Cancer Cells

Hyun S. Oh[1,4] Anabella Moharita,[1] Joseph G. Potian,[1] Ian P. Whitehead,[2] Jason C. Livingston,[1] Tammy A. Castro,[3] Prem S. Patel,[5] and Pranela Rameshwar[1]

[1]Department of Medicine, [2]Department of Microbiology and Molecular Genetic, and [3]Graduate School of Biomedical Sciences, University of Medicine and Dentistry of New Jersey-New Jersey Medical School, Newark, New Jersey; [4]Department of Clinical Pathology, Wonkwang Health Science College, Iksan, South Korea; and [5]Brookdale University Hospital and Medical Center, Department of Surgery, Brooklyn, New York

ABSTRACT

Breast cancer cells (BCCs) have preference for the bone marrow (BM). This study used an *in vitro* coculture of BCCs and BM stroma to represent a model of early breast cancer metastasis to the BM. The overarching hypothesis states that once BCCs are in the BM, microenvironmental factors induce changes in the expression of genes for cytokines and preprotachykinin-I (PPT-I) in both BCCs and stromal cells. Consequently, the expression of both PPT-I and cytokines are altered to facilitate BCC integration within BM stroma. Cytokine and transcription factor arrays strongly suggested that transforming growth factor-β (TGF-β) and c-myc regulate the expression of PPT-I so as to facilitate BCC integration among stroma. Northern analyses and TGF-β bioassays showed that stromal cells and BCCs influence the level of PPT-I and TGF-β in each other. In cocultures, PPT-I and TGF-β expressions were significantly ($P < 0.05$) increased and decreased, respectively. TGF-β and PPT-I were undetectable in separate stromal cultures but were expressed as cocultures. Two consensus sequences for c-myc in the 5′ flanking region of the PPT-I gene were shown to be functional using gel shift and reporter gene assays. Mutagenesis of c-myc sites, neutralization studies with anti-TGF-β, and transient tranfections all showed that c-myc is required for TGF-β-mediated induction of PPT-I in BCCs. TGF-β was less efficient as a mediator of BCC integration within stroma for c-myc-BCCs. Because the model used in this study represents BCC integration within BM stroma, these studies suggest that TGF-β is important to the regulation of PPT-I in the early events of bone invasion by BCCs.

INTRODUCTION

Many hormone-dependent cancers show preference for the bone marrow (BM; ref. 1). Different stimuli can cause responses in BM cells (2), indicating that the BM could be categorized as an organ with functionally "plastic" cells. Both clinical and experimental evidence suggests that cancer cells could take advantage of the plastic nature of BM cells, particularly stromal cells, to promote their own survival. The BM is host to relatively few hematopoietic stem cells that are responsible for replenishing the immune system throughout life (3). Because protecting these stem cells is perhaps the most important limitation in cancer treatments, understanding early BM invasion may be pivotal to eradicating certain cancers and improving current therapies.

Cancer metastasis to the BM is linked to poor prognosis (4, 5). It is generally thought that cancer cells survive within the bone (6). This study assumes that long before bone invasion is clinically detectable, and perhaps before the initial cancer diagnosis, malignant cells could enter and integrate into the BM stromal compartment and perhaps become involved in the interactions between BM stroma and hematopoietic stem cells, close to the endosteal areas of the BM (2, 7).

This study focuses on breast cancer (BC), which shows preference for BM (8). BC cells (BCCs) that metastasize to the BM have been thought to be derived from clones with multiple abnormalities. This premise has been challenged recently by Kittler *et al.* (9) who have shown that BCCs with relatively few mutations can enter the BM at low frequencies. These studies (9) are consistent with observed BC resurgence after 10 to 20 years of remission (10). Furthermore, whereas the BRCA genes link breast and ovarian cancers (11, 12), unlike BC, ovarian cancers do not show preference for the BM (12). This observation suggests that genes other than the BRCA genes are involved in BM metastasis.

Previous studies have elucidated the importance of the preprotachykinin-I gene (PPT-I) in early entry of BCCs in the BM (7). The PPT-I gene, linked to the endocrine system, has been associated with the biology of both BC and the BM (13, 14). *PPT-I* is a single copy, 7-exon gene that produces peptides that are conserved by evolution (15). *PPT-I* produces multiple peptides through alternate splicing and post-translational modification (15). In BM cells, PPT-I peptides interact with neurokinin (NK)-1 and NK-2, both G-protein coupled, 7-transmembrane receptors (16, 17). Coexpressions of NK-1 and NK-2 in BCCs are stimulated by PPT-I through autocrine mechanisms (13, 18).

This study has sought to elucidate the mechanisms by which the constitutively expressed PPT-I gene in BCCs mediates the integration of BCCs as part of the BM microenvironment, particularly among stromal cells (Fig. 1). This question is important because the answer would provide insight into mechanisms that allow BCCs to become part of the BM/hematopoietic microenvironment. Significantly, the 5′ flanking region of the PPT-I gene has two sites with consensus sequences that bind to the c-myc proto-oncogene (19, 20). Moreover, c-myc-mediated cell cycle progression of BCCs is resistant to the effects of transforming growth factor-β (TGF-β; 21). This study probes the roles of PPT-I, TGF-β, and c-myc in BC and extrapolates the data to understand how the associations of these three molecules could be involved in early entry of BC to the BM.

MATERIALS AND METHODS

Reagents, Cytokines, and Antibodies. FCS was purchased from Hyclone Laboratories (Logan, UT). Ficoll Hypaque and non-immune rabbit IgG were purchased from Sigma (St. Louis, MO). Recombinant interleukin (IL)-1α, TGF-β1, and rabbit anti-TGF-β were purchased from R&D Systems (Minneapolis, MN). FITC-goat antimouse IgG, phycoerythrin (PE) rat-antimouse kappa and PE-cytokeratin monoclonal antibody (mAb) were purchased from BD Bioscience (San Jose, CA). FITC-streptavidin was purchased from Vector

Received 10/3/03; revised 5/1/04; accepted 6/21/04.

Grant support: Grants CA-89868 and CA-097066 awarded by the National Cancer Institute and a grant awarded by Wonkwang Health Science College, Iksan, South Korea (H. S. Oh).

The costs of publication of this article were defrayed in part by the payment of page charges. This article must therefore be hereby marked *advertisement* in accordance with 18 U.S.C. Section 1734 solely to indicate this fact.

Note: H. S. Oh, A. Moharita, and J. G. Potian contribute equally to the study. This work was done at UMDNJ-New Jersey Medical School, Department of Medicine, Division of Hematology/Oncology.

Requests for reprints: Pranela Rameshwar, UMDNJ-New Jersey Medical School, MSB, Rm. E-579, 185 South Orange Ave, Newark, NJ 07103. Phone: 973-972-0625; Fax: 973-972-8854; E-mail: rameshwa@umdnj.edu.

Laboratories (Burlingame, CA). Two different clones of c-myc mAb were obtained from the following sources: Clone C-8 from Santa Cruz Biotechnology (Santa Cruz, CA) and Clone Ab-1 from Oncogene Research Products (San Diego, CA). Dynabead-Epithelial was purchased from Dynal Biotech (Oslo, Norway). Antifibroblast microbeads and FITC-fibroblast mAbs were purchased from Miltenyi Biotec (Auburn, CA). Non-immune rabbit IgG was obtained from Sigma Chemicals. Horseradish peroxidase-antimurine IgG was purchased from Amersham Life Science (Arlington Heights, IL).

Cell Lines. All cell lines were purchased from American Type Culture Collection (ATCC)[6] and propagated according to ATCC instructions. For group 1, tumorigenic cell lines were as follows: ZR-75–30/ATCC CRL-1504, ascites ductal carcinoma; BT-474/ATCC HTB-20, ductal carcinoma; T-47D/ATCC HTB-133, pleural effusion ductal carcinoma; MDA-MB-330, breast carcinoma from pleural effusion; DU4475/ATCC HTB-123 breast carcinoma; BT 483/ATCC HTB-121, ductal carcinoma; and SK-BR-3/ATCC HTB-30, pleural effusion adenocarcinoma. Each of the aforementioned cell lines constitutively expresses the PPT-I gene, as determined by immunoreactive substance P (7, 18). For group 2, non-tumorigenic/adherent-independent cells were as follows: MDA-MB-330/ATCC HTB-127. And for group 3, non-tumorigenic mammary epithelial cells were as follows: MCF12A/ATCC CR-10782; MCF-12F/ATCC CRL-10783; Hs578Bst/ATCC HTB-125; MCF 10A/ATCC CRL-10317; MCF-10^{-2}A/ATCC CRL-10781. Immunoreactive substance P was undetectable in this third group (7).

Primary Breast Tissue and Selection Method. Breast tissues were obtained from patients with stage IIIA or IIIB BC. At the time of surgery, patients were not subjected to chemotherapy or radiation. The use of breast tissues followed an approved protocol from the Institutional Review Board of University of Medicine and Dentistry of New Jersey, Newark Campus. Patient 7 tissue was obtained from Cooperative Human Tissue Network, University of Pennsylvania Medical Center (Philadelphia, PA). All tissues expressed the PPT-I gene and were diverse with respect to hormone receptor status (7).

The method to obtain maximal number of cells from breast tissues used a two-step procedure as described previously (7). Briefly, step 1 flushed the cells within the tissue by inserting culture media via a 1-cc syringe. Step 2 dislodged residual cells by gently teasing the tissue with serrated-end forceps. Fibroblasts were depleted by subjecting the cells to two positive selections with antifibroblast microbeads (Miltenyi Biotec, Auburn, CA). Two-color flow cytometry with FITC-antifibroblasts and PE-anticytokeratin verified fibroblast-depletion. Malignant cells, referred to hereafter as primary BCCs, were selected with a coculture method as described previously (7).

Modified Cells. PPT-I suppressed BCCs. PPT-I-cell lines and PPT-I-primary cells using stable transfection with an RNA interference-expressing vector were described previously (7). Non-tumorigenic cells in which PPT-I was stably expressed were described previously (7).

BM Stromal Cells. BM stromal cells were cultured from BM aspirates of healthy individuals as described previously (17). The use of BM aspirates followed the guidelines of a protocol approved by the Institutional Review Board of University of Medicine and Dentistry of New Jersey-Newark Campus. At confluence, non-adherent cells were removed and trypsin-sensitive cells were passed at least five times. α-MEM (Sigma) served as the base medium for the stromal cultures. Flow cytometry indicated that >99% of passage 5 cells were positive for antifibroblasts.

Cocultures of BCCs and BM Stroma. Cocultures of BCCs and BM stromal cells were established as described previously (7). Briefly, cultures were initiated with equal numbers of BCCs (primary or cell lines) and BM stroma in stromal media. At cell confluence, the BCCs were positively selected with anticytokeratin-conjugated Dynabeads. Flow cytometry determined >99% purity for each of the selected cell subsets. BCCs were analyzed with PE-cytokeratin mAb and stromal cells with FITC-fibroblasts mAb. Nonspecific labeling was determined in parallel labeling with PE- and FITC-conjugated isotype control. Following isolation from cocultures, BCCs were able to survive in stromal media (no exogenous growth supplement) for up to 1 week.

Modified Cocultures. Cocultures performed with PPT-I- (by RNA interference) BCCs and non-tumorigenic cells (PPT-I-) did survive (7). A modified coculture was performed with PPT-I-BCCs or non-tumorigenic cells and stroma in the presence or absence of different $\log_{10}$-fold concentrations of exogenous TGF-β, between 1 and 10 μg/ml.

The corollary of the above cocultures was performed with unmanipulated BCCs (PPT-I+) or non-tumorigenic mammary cells with PPT-I stably expressed (7). Cultures were performed in the presence or absence of various concentrations of rabbit antihuman TGF-β1. Control cultures contained equivalent amounts of non-immune rabbit IgG. To be sure that TGF-β was neutralized, at different times, supernatants were collected and then subjected to the following procedure: immune complexes of TGF-β-anti-TGF-β and free anti-TGF-β were cleared with protein G Sepharose beads. After this, the supernatants, free of immune-complexes were assayed for bioactive TGF-β (see below).

Northern Analysis. Northern analyses for steady-state PPT-I mRNA in BM stroma and BCCs were performed as described previously (22). To be sure that adequate RNA was obtained from each cell subset, the coculture was established with 10 to 15 replicates in 25-cm^2 flasks. Total RNA was extracted from BM stroma or BCCs using RNeasy mini kit (Qiagen, Valencia, CA). Samples, 10 μg of each, were separated by electrophoresis in 1.2% agarose. RNA was transferred to nylon membranes (S & S Nytran, Keene, NH) and then hybridized with β-PPT-I-specific cDNA probe, randomly labeled with 3,000 Ci/mmol [α-^{32}P]-dATP (DuPont/NEN, Boston, MA). Probes were labeled with the Prime-IT II random primer kit (Stratagene, La Jolla, CA). To normalize RNA loading, membranes were stripped and reprobed with cDNA for 18S rRNA. Hybrids were detected by exposures in a phosphoimager cassette (Molecular Dynamics, Sunnyvale, CA), which was scanned at different times from 6 to 24 hours with the Typhoon 9410 Molecular Imager phosphoimager system (Molecular Dynamics). The PPT-I cDNA probe was prepared by revere transcription-PCR using primers that span exons 3 to 7 (accession number x54469, +218/+532). The RNA template for reverse transcription-PCR was derived from BM stroma stimulated for 16 hours with 10 ng/ml IL-1α.

Microarray for Transcription Factors. Cocultures of BCC (primary cells and cell lines) and BM stroma were screened for transcription factors (TF) using TranSignal Protein/DNA Array (Panomics, Redwood City, CA). The method followed manufacturer's protocol. Briefly, BCCs and stromal cells were isolated as described above, and nuclear extracts were immediately prepared using CellLytic Nuclear extraction kit (Sigma). Cells were lysed with 5 times the packed cell volume with 1× Lysis buffer containing protease inhibitor mixture (Sigma). Cells were disrupted by a 15-minute incubation at room temperature. The nuclear fraction was pelleted by centrifugation at 10,000 × *g* for 20 minutes. Nuclear extracts were prepared with extraction buffer containing protease inhibitors and then centrifuged at 20,000 × *g* for 10 minutes. Protein concentrations were quantitated with an assay kit purchased from Bio-Rad (Hercules, CA).

Nuclear extracts (5 μg) were incubated with biotin-DNA probe mix (provided in the kit) for 30 minutes. Protein-DNA complexes were selected by agarose (2%) gel electrophoresis. Proteins were eliminated from the complex and the biotin-DNA was used to hybridize the membranes with consensus-binding sequences for TF. After this step, membranes were incubated with streptavidin-alkaline phosphatase conjugate. Biotin-conjugates were detected by chemiluminescence (enhanced chemiluminescence system, NEN Life Sciences, Boston, MA). The densitometric scans for the positive controls on the membranes were arbitrarily assigned 2 and negative spots were assigned 0.

Western Blots. Proteins (10 μg) were separated by electrophoresis on 12% SDS-PAGE and then transferred to nylon membranes (NEN Life Sciences) for 1 hour at 60 V. Membranes were incubated consecutively with anti-c-myc (1:2000) overnight at room temperature and with horseradish peroxidase-antimurine IgG for 2 hours at room temperature. Hybrids were detected by chemiluminescence as above. The molecular weight of developed bands was compared with Kaleidoscope Prestained standards (Bio-Rad Laboratories, Hercules, CA).

Microarrays for Cytokines. Cytokines were screened by microarrays using culture media from confluent BCCs that were unmanipulated (PPT-I+) or stably transfected with the RNA interference plasmid, pPMSKHI-PPT-I (PPT-I-; 7). At 24 hours before assay, culture media from confluent cultures were replaced with fresh media. At collection, media were immediately centrifuged and then stored as aliquots in siliconized tubes at −80°C. Whole cell extracts were prepared from the same cultures by repeated freeze-thaw in PBS (pH 7.4)

[6] www.atcc.org.

containing protease inhibitor mixture at 1:2000. Extracts were cleared by centrifugation and cell-free extracts stored as culture supernatants.

Human cytokine protein array II was purchased from Ray Biotech, Inc. (Norcross, GA) and used according to the manufacturer's instructions. Briefly, membranes were blocked with 5% BSA and were then washed with 1× Tris-buffered saline/0.1% Tween followed by two 5-minute washes with Tris-buffered saline. Membranes were incubated with fresh culture media, culture supernatants, cell extracts, or culture supernatants + cell extracts. After this, membranes were incubated for 1 hour with biotin-conjugated anticytokines (provided with the kit) and then developed with horseradish peroxidase-streptavidin and chemiluminescence.

Quantitation of Bioactive TGF-β. Bioactive TGF-β was quantified with CCL64 cells as described previously (23). CCL64 cells at 10^4/ml were resuspended in assay medium (RPMI 1640 and 10% FCS), and 0.5 ml added to 24-well tissue culture plates. After 24 hours of incubation at 37°C, unknowns were added to wells in triplicates at the following three undiluted volumes: 25, 50, and 100 μl. At day 3, viable cells were counted and TGF-β levels were determined with a standard curve that was established with TGF-β1 concentrations ranging from 0.001 ng/ml to 10 ng/ml. Samples with ≥20 ng/ml TGF-β were reanalyzed in the presence or absence of neutralizing rabbit anti-hTGF-β. This antibody was shown previously to exhibit specificity for the -β1 isoform of TGF-β (23).

***In situ* Hybridization for PPT-I mRNA.** *In situ* hybridization for PPT-I mRNA was performed with a mixture of three biotin-conjugated oligonucleotides specific for β-PPT-I, as described perviously (18). Briefly, cocultures of BCCs and BM stroma were established on coverslips placed in 35-mm Petri dishes. At confluence, cells were permeabilized with PBS-Tween and then hybridized overnight at 37°C with 20 μmol/L of oligonucleotide mixture. After this, cells were incubated with 1:1000 dilution of FITC-streptavidin for 2 hours. The following controls were labeled in parallel: cells incubated with FITC-streptavidin alone, cells hybridized with scrambled oligonucleotides, and cells pretreated with RNase and then incubated with antisense oligonucleotides. Immediately after staining, cells were examined for fluorescence intensity with an OlympusProbis microscope.

Electrophoretic Mobility Shift Assay. Electrophoretic mobility shift assay (EMSA) for c-myc binding was performed as described previously (19). Double-stranded oligonucleotides were synthesized with Cy3 at the 5′ ends. DNA sequences spanned +421/+441 and +634/+654 of the 5′ flanking region of the PPT-I gene (accession number AF252261). The changes in nucleotide sequences in both c-myc regions are shown in Table 1. Double-stranded probes were prepared with 2.5 μg of the forward and reverse oligonucleotides. Reaction mix consisted of 2.5 μg of double-stranded DNA, 3 μg of poly(dI·dC) (Sigma) and 25 μg of proteins. Parallel reactions contained three different c-myc mAb, each at 1:20 dilution. Cy3 was detected by scanning the gels on the Typhoon 9410 Molecular Imager.

Transfection and Reporter Gene Assay. Experimental vectors with luciferase-reporter gene inserts were cotransfected with pβ-gal-Control (0.5 μg each) in 80% confluent cells using SuperFect (Qiagen). At 48 hours, cell-free lysates were prepared as described previously (19). Luciferase and β-gal activities in 10 μl of extracts were quantitated using the Luciferase assay system (Promega, Madison, WI) and the Luminescent β-galactosidase detection kit II (BD Bioscience Clontech, Palo Alto, CA), respectively. The ratios of Luciferase/β-gal in cells transfected with vector alone were normalized to 1 and ranged between 0.18 and 0.19. β-Gal activities ranged between 100- and 1,000-relative light units. Cotransfectants were intermittently stained with X-Gal (Life Technologies, Inc.), and the number of blue cells was counted to ensure that the DNA is taken up by >80% of the transfectants. On the basis of the transfection efficiency and error bars for each experimental point (refer to Figs), we observed no evidence of donor variability. Because cytokines activate β-gal promoter, luciferase activities in cultures stimulated with cytokines were presented per microgram of total protein, and the levels were normalized with cells transfected with vector alone. Total protein was determined with a kit purchased from Bio-Rad.

Table 1 *Wild-type and mutant c-myc sites in the PPT-I gene*

c-myc	Position	Sequence
Wild-type site a	+421/+441	5′ aaggagag **gggaggg** ggcgtc 3′
Mutant site a		***t*ggc*g*cg**
Wild-type site b	+634/+654	5′ gagaatgt **cacgtg** ggtctgg 3′
Mutant site b		***t*aaggg**

NOTE. Bold, consensus sequences for c-myc based on the 5′ flanking region of PPT-I, accession number AF252261. Mutant nucleotides, italics/underlined.

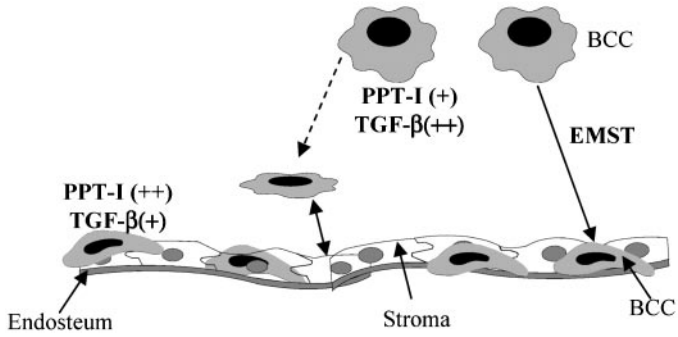

Fig. 1. Diagram of hypothesis shows BCCs entering the BM cavity. As the cells approach the endosteal region where the stromal cells are located, they EMST (7). PPT-I is increased (++) as the BCCs form contact with the stromal cells, whereas TGF-β (+) levels are decreased. Cytokines and PPT-I produced in BCCs mediate changes in the stromal cells (*shown by double headed arrows* between stroma and BCCs close to the endosteum).

Vectors. The 5′ flanking region of PPT-I was cloned previously and analyzed (19). Figure 3*A* shows the regions of various inserts as cartoons. pGL3-PPT-I-1.2: 740 bp upstream of exon 1, exon 1, and parts of the 5′ region of Intron 1; pGL3-PPT-I/N0: 740 bp upstream of exon 1 with consensus sequences for c-myc, *sites a* and *b*; pGL3-PPT-I/N3: 5′ deleted fragment of PPT-I/N0 with consensus sequence for c-myc, *site b*; pGL3-PPT-I/Exon 1: exon 1.

Site-directed mutagenesis of the two c-myc sites was done with a mutagenesis kit from Stratagene as described previously (19). The following designations were given to c-myc mutants: *site a*, pGL3-PPT-I/N0mut a; *site b*, pGL3-PPT-I/N0mut b; *sites a* and *b*, pGL3-PPT-I/N0mut ab (Table 1). pRC-CMV-hu-myc, kindly provided by Dr. Stephen Hann, Vanderbilt University, contains the full-length human c-Myc cDNA under the control of a cytomegalovirus promoter.

Data Analyses. In all studies, data performed with cell lines and cells of patients were similar. Therefore the results of cell lines were analyzed together. Similar analyses were done for experiments with cells from patients. Statistical evaluations of the data were done by using ANOVA and Tukey-Kramer multiple comparisons test. A P value of < 0.05 was considered significant.

RESULTS

This study is based on the "hypothetical" model, shown in Fig. 1. The model depicts BCCs entering the BM express PPT-I (18) at an early phase of cancer invasion. The BCCs move toward the endosteal region where they begin to integrate among stromal cells (7). In the stromal microenvironment, the BCCs undergo phenotypic and functional transition, termed epithelial-to-mesenchymal-to-stromal transition (EMST; ref. 7). Interaction between BCCs and BM stromal cells induce molecular changes in each other resulting in altered expressions of PPT-I and TGF-β in each cell subset. Consequently, the BCCs acquire quiescence within the BM stromal compartment. Importantly, this hypothesis suggests an altered role for TGF-β in BCC-stromal interaction than its role in normal BM stromal cells in which PPT-I is minimally induced by TGF-β (Fig. 2*C*), as compared with a known stimulator of PPT-I such as IL-1α (19; Fig. 2*C*).

Relative Expression of PPT-I in BM Stroma and BCCs before and after Coculture. Studies show that the PPT-I gene is important for the integration of BCCs within the stromal compartment of the BM (7). Although PPT-I is constitutively expressed in BCCs (7, 13, 18), it is unclear if similar expression occurs when BCCs are in a microenvironment with BM stroma. To this end, we studied the expression of PPT-I in BM stroma and BCCs (six cell lines and six

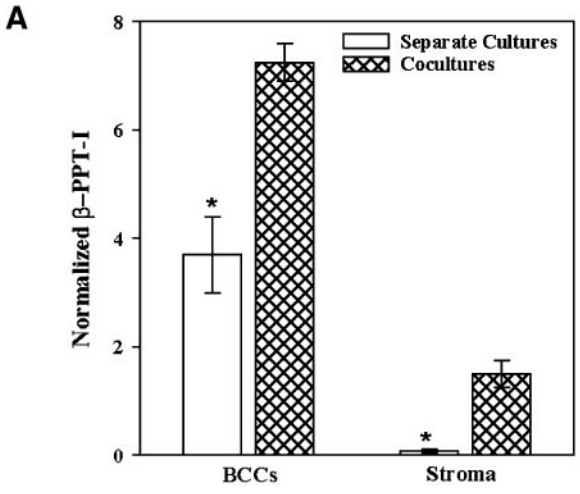

C

Stimuli	Molecules of β-PPT-I/ μg total RNA	Substance P (pg/ml)
TGF-β	30±5	15±4
IL-1α	4055±34	453±12
Media	12±3	<2

Fig. 2. Expression of PPT-I in BCCs and BM stroma. *A*, BCCs were positively selected from confluent cocultures, and total RNA from both cell subsets (BCCs and stroma) were analyzed for β-PPT-I by Northern analyses. Band intensities were normalized with 18S rRNA. The ratios of β-PPT-I in cocultures are the mean ± SD of 12 experiments: six BC cell lines and six primary BCCs, presented together. Each BCC was tested with a BM stroma from a different donor, $n = 12$. *B*, confluent cocultures were labeled for PPT-I mRNA by *in situ* hybridization with biotin-conjugated oligonucleotides, specific to three different parts of β-PPT-I. Hybrids were detected with FITC-streptavidin. Figure represents five different experiments.

primary cells) before and after coculture. In cocultures, normal breast epithelial cells do not survive, leaving only malignant cells (7). By Northern analyses, the densities of normalized β-PPT-I in BCCs were found to be increased 2-fold in coculture compared with similar cultures in which BCCs were cultured separately (Fig. 2*A*; 4 ± 1.1, $n = 12$). PPT-I mRNA levels were constant up to 4 months in unmanipulated cocultures (not shown). In stromal cells, β-PPT-I levels were changed from minimal intensity in separate cultures to ~1.5-fold in cocultures (Fig. 2*A*). The observation of low PPT-I in separate cultures of stroma is consistent with other studies, which show that PPT-I expression in stroma requires cell stimulation (19; Fig. 2*C*).

The studies shown in Fig. 2*A* required that the cultures undergo major experimental manipulations to acquire pure populations of each subset. Thus, to exclude the possibility that the observations in Fig. 2*A* were artifacts of manipulation, we analyzed the cells for PPT-I mRNA by *in situ* hybridization while the cells were in cocultures. Figure 2*B* shows brighter fluorescence for PPT-I in confluent cocultures. Colabeling with cell-specific antibodies (PE-cytokeratin mAb and FITC-fibroblasts mAb) showed that PPT-I was expressed in both stroma and BCCs (not shown). This section demonstrates that PPT-I expression in BCC and BM stroma are altered when the subsets of these two cells are in contact with each other. Furthermore, the increases in PPT-I expression in both stroma and BCCs in cocultures were significant ($P < 0.05$) when compared with similar cells cultured separately.

Activities of the 5′ Flanking Regions of PPT-I in BM Stroma and Breast Cells. From the preceding observations with malignant cells (Fig. 2), we could not extrapolate how PPT-I is regulated in non-tumorigenic mammary epithelial cells. Because PPT-I expression was different in coculture BM stroma and BCCs (Fig. 2), it was important to ask whether PPT-I shows tissue-specific regulation in breast and BM cells. This question was addressed with the following cells lines: seven different BCCs (regardless of c-myc status), five different non-tumorigenic breast cells, and BM stroma from 10 different donors. Cells were transfected with pGL3-PPT-I/1.2, pGL3-PPT-I/N0, or PPT-I-Exon 1 (Fig. 3*A*). Because exon 1 is untranslated and might have regulatory sequences that confer tissue specificity, we included fragments of PPT-I/1.2. The trends were similar for reporter gene activities in BCCs, stroma and non-tumorigenic breast cells (Fig. 3*B*). However, luciferase activities were significantly ($P < 0.05$) increased for non-tumorigenic breast cells as compared with BCCs and stromal cells. These data indicate that PPT-I exerts tissue specificity with regards to the efficiency of reporter gene activity, although the trend for reporter gene activity was similar in BM stroma, BCCs and non-tumorigenic breast cells.

Activation of PPT-I/1.2 and PPT-I/N0 in Cocultures. Studies in this section used the reporter gene constructs to understand why PPT-I expressions were changed in both BCCs and BM stroma following cocultures (Fig. 2). The activity of exon 1 as separate gene insert was only increased in non-tumorigenic cells (Fig. 3*A*). Because these cells do not survive in cocultures, this section focused on PPT-I/1.2 and PPT-I/N0 (7). Cocultures were transfected with pGL3-PPT-I/1.2 or pGL3-PPT-I/N0. After 48 hours, BCCs were positively selected and

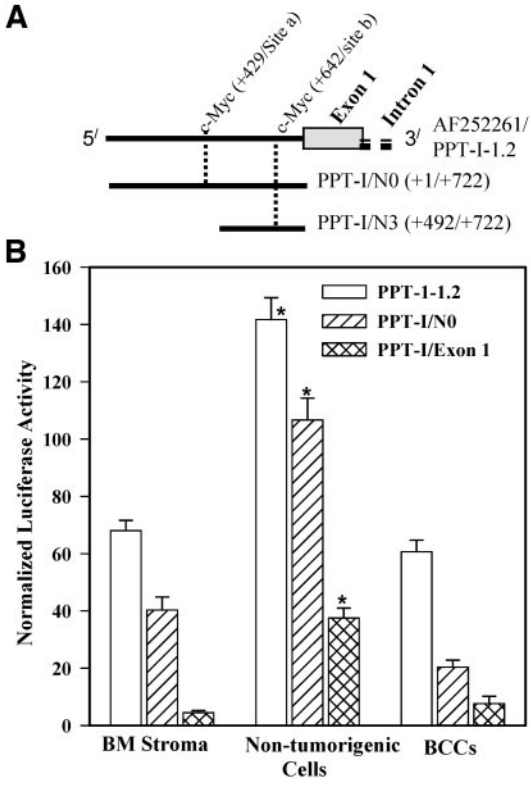

Fig. 3. Luciferase activities of PPT-I-reporter genes in different cell types. *A*, relative sizes and positions of gene-specific inserts (19) and the relative locations of c-myc-binding sites. *B*, pGL3-PPT-I-1.2, -PPT-I/N0, or -Exon 1 were cotransfected with pβ-gal in the following: BC cell lines, non-tumorigenic cells, BM stroma. Luciferase activities were normalized with β-gal. The results presented as the mean ± SD of normalized luciferase are as follows: BM stroma ($n = 40$ different donors), non-tumorigenic cells ($n = 20$: five cell lines; four repeats), and BCCs ($n = 28$: 7 different cell lines; four repeats). *, $P < 0.05$ *versus* similar transfectants in BM stroma or BCCs.

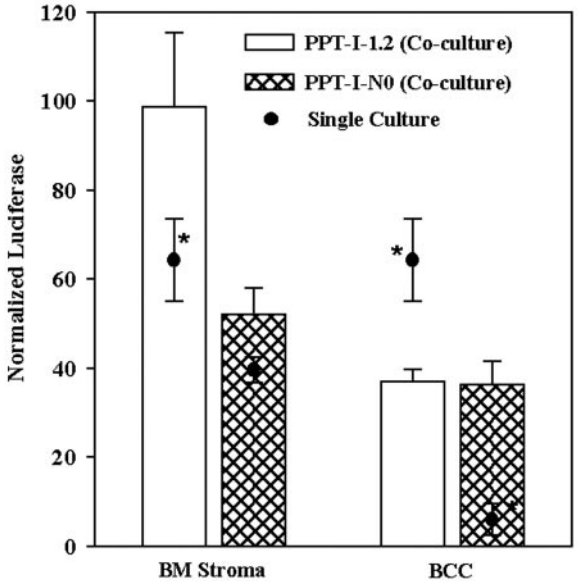

Fig. 4. Activities of PPT-reporter gene constructs in cocultures. pGL3-PPT-I-1.2 or -PPT-I/N0 were cotransfected with pβ-gal in cocultured BC cell lines, regardless of c-myc expression. Each cell subset was isolated and then analyzed for luciferase activities. Normalized luciferase was performed as for Fig. 3. Each experimental point is presented as the mean ± SD, $n = 21$ for seven BCCs, each assayed with stroma from three different donors. ∗, $P < 0.05$ *versus* activities in the same cell subsets from cocultures.

cell lysates from BCCs and the negative subset (stroma) were analyzed for reporter gene activities. Except for BCCs with PPT-I-1.2, luciferase activities were significantly ($P < 0.05$) increased in all other cocultures compared with separate cultures (Fig. 4, *vertical bars versus solid circles*). At the molecular level, these results suggest contact between BCCs and BM stroma induces differences in PPT-I regulation.

Cytokine Profiles in BM Stroma and BCC: Coculture *versus* Separate Cultures. Because cytokines influence the expression of PPT-I (24), the next set of studies determined their expressions in coculture because this information might begin to provide insights in the altered expressions of PPT-I in cocultures (Fig. 2). Microarrays studied cytokine expression in cocultures established with six BCCs (three cell lines and three primary cells). Each BCC was studied with stroma from a different BM donor. Because stromal cells produce extracellular matrix proteins that could mobilize cytokines, whole cell extracts were included in the analyses. Each experiment was analyzed with the following samples: culture media (released cytokines), whole cell extracts (cell-associated cytokines), and combinations of culture media and cell extracts (released + cell-associated). Similar analyses used samples from single cultures of stroma or BCCs.

Microarray membranes were scanned, and the densitometry of each spot was assessed. These results are presented as the ratio of the value in samples taken from BCCs cultured alone to the value in samples taken from coculture. Factors were classified as either cytokines (Fig. 5*A*) or chemokines (Fig. 5*B*). Factors showing similar ratios were plotted together and are presented as the mean ± SD ($n = 6$) ratios (BCCs alone/cocultures). Thus, the densitometric ratios are inversely proportional to cytokine production in cocultures. Among the cytokines in the arrays, three cytokines showed marked increases in coculture (IL-6, IL-1α, and stem cell factor) whereas a high density of platelet-derived growth factor was detectable only in cocultures. Interestingly, insulin-like growth factor linked to bone resorption by BCCs was unchanged in the cocultures (6). The chemokines growth-related oncogene and monokine induced by IFN-γ were also increased. High production of TGF-β was retained, although its level was decreased when compared with cells cultured alone. To verify that the cytokine array data represent the relative changes in cytokines, we selected two cytokines (stem cell factor and stromal-derived factor-1α) for quantitation by ELISA. The results for BCCs/coculture are similar to the microarray data: stem cell factor = 8 ± 3 pg/ml/40 ± 5 pg/ml; stromal-derived factor-1α = 55 ± 3 pg/ml/28 ± 1 pg/ml.

TF and TGF-β in BCCs and BM Stroma: Cocultures *versus* Separate Cultures. The presence of particular TF could be linked to specific cytokines. Thus, by scanning nuclear extracts of cocultures for TF, we would be able to identify cytokines relevant to PPT-I as a facilitator gene in BCC integration within BM stroma (7). Nuclear extracts from BCCs or BM stroma (cocultures and separate cultures) were analyzed using TF microarrays. Selected results, shown in Table 2, indicate that Smad, Smad-binding proteins, and c-myc were increased in BCCs after coculture. Interestingly, E2F, which has been linked to cell proliferation, was undetectable in cocultures. This observation is consistent with contact inhibition in the growth of BCC and stromal cells at confluence (7). Smad proteins are linked to TGF-β cell signaling (25). Because BCCs are resistant to TGF-β, the link between TGF-β and the PPT-I gene is particularly interesting. The level of TGF-β might be pivotal in explaining BM homeostasis *versus* disruption when BCCs enter the BM (26, 27).

Microarray analyses were repeated with the following modification; BCCs and stroma were separated at cell confluence. The production of cytokines from each cell subset was determined by replating separately for 24 hours in the coculture media. The changes in TGF-β, as determined by densitometric scans of the microarrays, are

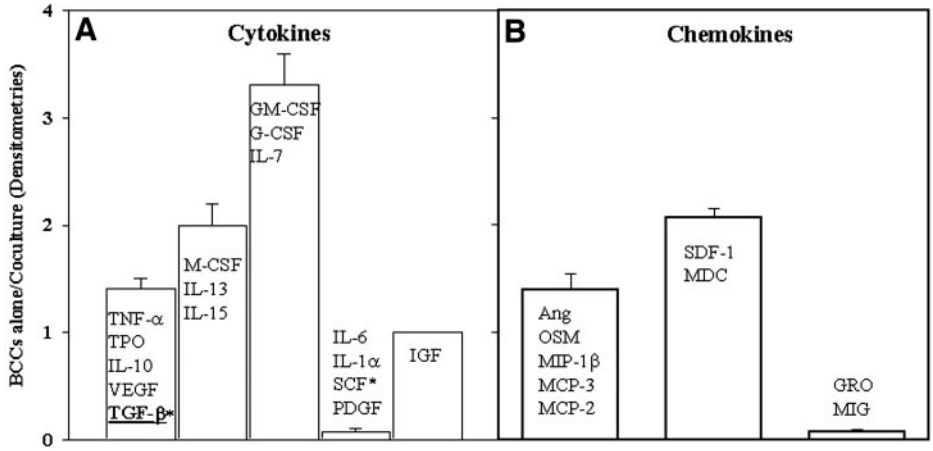

Fig. 5. Cytokine profile in BCC-BM stroma cocultures. Supernatants and cell extracts from cocultures were analyzed with protein microarrays. The spots were analyzed by densitometric scans and the data represented as the ratios (mean ± SD, $n = 6$) of BCC as separate cultures/cocultures, mean ± SD, $n = 6$ for three different BC cell lines and primary BCCs from three different patients. ∗, Undetectable in PPT-I-suppressed BCCs.

Table 2 *Transcription factors in BCCs: cocultures versus separate cultures.*

TF	BCCs/ separate	BCCs/ coculture	Stroma/ separate	Stroma/ coculture
p53	2	1	0	0
E2F1	2	0	0	0
c-Myb	1	0	0	0
Myc-Max*	1	2	0	0
SmadSBE/Smad	0	1	0	0
IRF-1	1	0	1	0
CREB	1	2	0	2

NOTE. BCC (three cell lines and two primary cells) were cultured with BM stroma or as separate cultures. At cell confluence, BCCs were positively selected and nuclear extracts immediately isolated and analyzed with transcription factor membranes. The changes in transcription factors (TF) shown in the Table were observed for all cultures studied. The densitometic scans for the internal positive controls were arbitrarily assigned 2 and the negative controls 0. The two extremes were used to normalize the densities of unknown samples. The techniques are described in Materials and Methods.

* Detected at similar densities in PPT-I-suppressed BCCs.

consistent with the bioactive levels of TGF-β (Fig. 6). In BCCs, TGF-β levels were changed from 125 ± 8 pg/ml as separate cultures to 25 ± 3 pg/ml in cocultures. For stroma, the levels were changed from <5 pg/ml to 45 ± 5 pg/ml in cocultures. The results of bioactive TGF-β are the mean ± SD of 14 BCCs (seven primary and seven cell lines). Each BCC type was assayed with stromal cells from a different donor. The results show changes in TGF-β production in both BCCs and BM stroma following cocultures.

Interactions between c-myc and Consensus Sequences in PPT-I/N0. The next set of studies sought to link the changes in TGF-β production in cocultures with the PPT-I gene (Figs. 2, 4, and 6). This question is important because BCCs have been shown to be resistant to TGF-β (27). Furthermore, c-myc suppression in cancer cells is resistant to the activation of Smad proteins by TGF-β (25). The 5′ flanking region of PPT-I has two potential binding sites for c-myc (Fig. 3*A*). We first investigated whether these sites are functional using gel-shift and supershift assays with nuclear extracts from c-myc$^+$ BCCs. The extracts were verified for immunoreactive c-myc by Western blots (Fig. 7*A*; representative blots for BCCs, three cell lines and three primary cells). Supershifts were observed when the oligo-cell extract reactions were incubated with a mixture of three different clones of c-myc mAb (Fig. 7*B*).

Role of c-myc Interacting Sites in the Activation of PPT-I. Studying the role of c-myc sites in PPT-I activation requires the first set of studies done with normal cells. To this end, BM stromal cells from healthy donors were cotransfected with PPT-I/N0 (two c-myc regions) or PPT-I/N3 (one c-myc region) reporter vectors and pRC-CMV-hu-myc (expression vector). Cell transfection was normalized with β-gal. Figure 7*C* shows the mean ± SD of normalized luciferase for seven different experiments. The results show that cotransfection with c-myc enhances reporter gene activities.

After establishing the importance of c-myc sites in PPT-I activation in normal stromal cells, studies were then extended to BCCs. One or both c-myc sites (double mutants) were mutated and then cotransfected into c-myc$^+$ BCCs or c-myc$^-$ BCCs. Each category of BCCs was studied with seven different cell types (four cell lines and three primary cells). For c-myc$^+$ BCCs, mutation of one site did not affect the activities of PPT-I/N0 (Fig. 7*D*). However, double mutations resulted in significant ($P < 0.05$) reduction in luciferase activities (Fig. 7*D*). Cells that were c-myc$^-$ showed no change in PPT-I/N0 activities, regardless of mutations (Fig. 7*D*). These studies show that the 5′ flanking region of PPT-I contains two functional c-myc sites that are relevant to its activities. Furthermore, the numbers of c-myc sites are irrelevant to PPT-I activities in BCCs.

Effects of TGF-β1 in the Activities of PPT-I Promoter in c-myc$^+$ BCCs. Because TGF-β levels are changed after coculture (Fig. 6), we hypothesized that this cytokine might be linked to PPT-I and thus relevant to BCC integration among stromal cells (7). We addressed this question by first investigating whether c-myc is relevant to PPT-I-reporter gene activities and, if so, to determine the role of TGF-β in c-myc-mediated activities. c-myc$^+$ BCCs (three different cell lines and three different primary cells) were transfected with pGL3-PPT-I/N0 (wild-type c-myc *sites a* and *b*, Fig. 3*A*) or pGL3-PPT-I/N3 (wild-type c-myc *site b*, Fig. 3*A*). Stimulation of transfectants with 10 ng/ml of TGF-β1 led to significant ($P < 0.05$) activation of PPT-I/N0 and PPT-I/N3 (Fig. 8*A*). Overall, TGF-β induced the activities of PPT-I fragments in c-myc$^+$ BCCs.

Does TGF-β Activate PPT-I-Reporter Gene Activities via c-myc? Because the studies shown in Fig. 8*A* did not prove a cause-effect relationship between c-myc and TGF-β in PPT-I activities, we addressed this question by transfecting PPT-1/N0 in c-myc$^-$ BCCs and then stimulated the transfectants with 10 ng/ml of TGF-β1. The status of c-myc expression in BCCs was verified by Western blots. In contrast to increased luciferase activity for c-myc$^+$ BCCs stimulated with TGF-β1 (Fig. 8*A*), there was significant ($P < 0.05$) reduction for c-myc$^-$ BCC by 4-fold (Fig. 8*B*).

Role of Endogenous TGF-β in the Activation of PPT-I in c-myc$^+$ BCCs. Because exogenous TGF-β1 induced PPT-I-reporter gene activities in c-myc$^+$ BCCs (Fig. 8*A*), we next studied whether PPT-I could be regulated by autocrine stimulation with endogenous TGF-β (Fig. 6). BCCs (c-myc$^+$) were transfected with PPT-I/N0 containing wild-type or mutant c-myc *sites a* and *b*. Mutations were verified by gel shift assays with c-myc protein (Fig. 7*C*). Endogenous TGF-β was neutralized by culturing the transfectants in the presence of various concentrations of anti-TGF-β, 1 to 50 ng/ml. Control cultures contained equivalent concentrations of non-immune rabbit IgG. Anti-TGF-β at ≥2 ng/ml neutralized active TGF-β as determined by undetectable levels in the culture supernatants. The results showed that neutralization of TGF-β led to significant ($P < 0.05$) decreases in luciferase activities for wild-type c-myc (Fig. 8*C*, *open versus diagonal bars*). Decreases were similar in parallel studies in which c-myc sites were mutated (Fig. 8*C*, *hatched bar*). Anti-TGF-β showed no effect in studies with mutant c-myc (Fig. 8*C*, *horizontal*

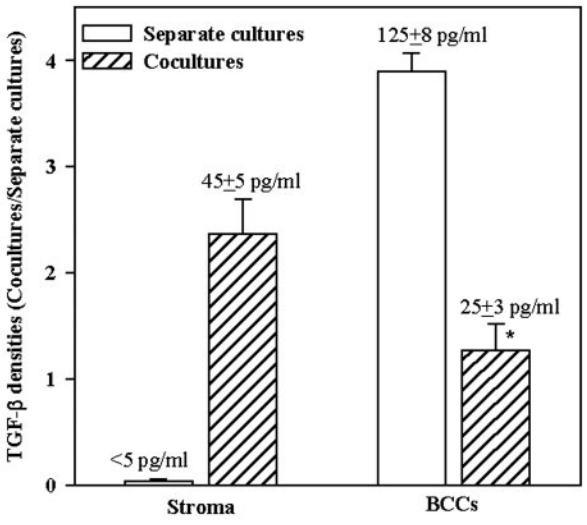

Fig. 6. TGF-β production in BM stroma and BCCs. Cells from cocultures were separated and then subcultured separately. After 24 hours, culture supernatants and cell extracts were analyzed with cytokine microarrays. The results are presented as fold changes in cocultures/mean densities ± SD of six different experiments (three cell lines and three primary BCCs). The equivalent bioactive TGF-β1 levels in each sample are presented as the mean ± SD (pg/ml, $n = 12$) for cultures performed with BCCs: seven cell lines and five primary BCCs. The total levels of TGF-β in unseparated cocultures were 77 ± 5 pg/ml ($n = 12$). Details of the techniques are described in Materials and Methods. *, $P < 0.05$ *versus* BCC cultured alone.

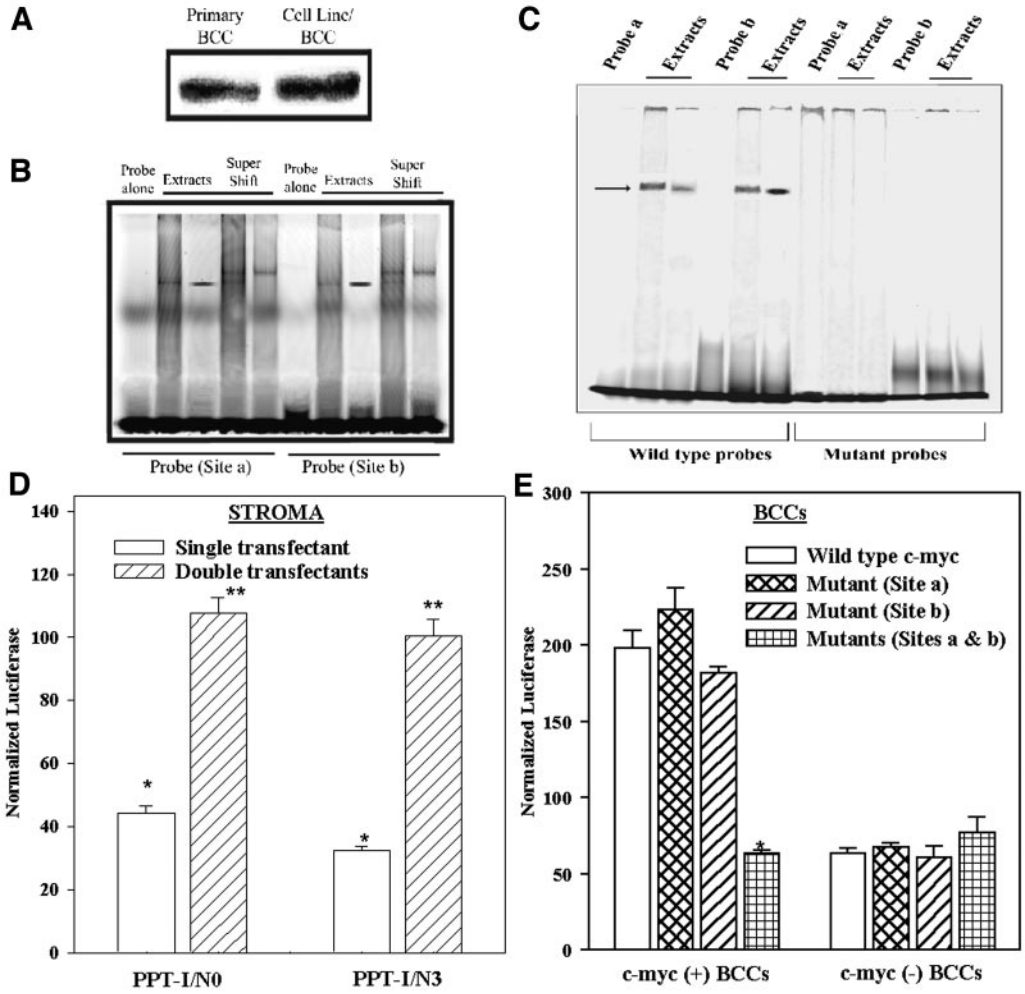

Fig. 7. Role of c-myc in the activities of PPT-I. *A*, representative Western blots for c-myc protein in BCCs (cell lines and primary cells). *B*, representative EMSA show interactions between c-myc and the respective consensus regions (*Sites a* and *b*) in PPT-I/N0. *C*, EMSA with mutant c-myc sites. *D*, BM stromal cells from healthy donors were transfected (*Single transfectant*) with pGL3-PPT-I/N0 (c-myc, *sites a* and *b*) or PPT-I/N3 (c-myc *site b*). Parallel studies were performed by cotransfecting with pRCCMV-hu-myc (double transfectants). The results are the mean ± SD of seven experiments, each with a different BM donor. *, $P < 0.05$; **, $P > 0.05$. *E*, BCCs were divided into c-myc$^+$ and c-myc$^-$ cells. Each group consisted of three cell lines and three primary cells. Cells were transfected with pGL3-PPT-I/N0 containing wild-type or mutant c-myc sites. Luciferase activities were normalized as for Fig. 3, and the activities are presented as the mean ± SD, $n = 6$. *, $P < 0.05$ *versus* each experimental point within the c-myc$^+$ group.

versus hatched bar). The results for non-immune rabbit IgG were similar to studies with wild-type c-myc and were therefore plotted in the same bar (Fig. 8*C*, *open bar*). It should be noted that despite the double mutations of the two c-myc sites in PPT-I/N0, luciferase activities were >50-fold over background/vector (Fig. 8*C*). The results show that endogenous TGF-β is partly responsible for c-myc-mediated activation of PPT-I/N0 in BCCs.

TGF-β in the Integration of BCCs within BM Stroma: Link with PPT-I and c-myc. The next set of studies was designed to further elucidate the potential interaction among PPT-I, c-myc, and TGF-β in the integration of BCCs within BM stroma (7). Cocultures were established with BCCs (c-myc$^+$ or c-myc$^-$) and BM stroma in the presence or absence of varied concentrations of TGF-β Ab. Parallel cultures containing non-immune rabbit IgG were used for non-specific effects. At different times after cocultures, the total numbers of cytokeratin (+) cells were counted with positively selected cells. At the time of cell counting, active TGF-β levels were assayed to verify neutralization by the antibody. The data from experiments with non-immune rabbit IgG and untreated cultures were similar and were therefore combined (Fig. 9, *solid circle*).

Neutralization of TGF-β showed significant ($P < 0.05$) reduction in the numbers of c-myc$^+$ BCCs (Fig. 9*A*, *solid square*) compared with cultures with non-immune/untreated cocultures (Fig. 9*A*, *solid circle*). Cocultures with c-myc$^-$ BCCs showed significant ($P < 0.05$) reduction in cell growth at week 4 (Fig. 9*B*, *solid circle versus solid square*). PPT-I-BCCs do not expand in cocultures (7). Furthermore, by microarray studies, we showed that TGF-β is not produced in PPT-I-BCCs, but is induced in PPT-I expressing non-tumorigenic cells (7). We therefore sought to determine whether TGF-β1 supplementation would facilitate the formation of cocultures with PPT-I-BCCs. The results show that whereas TGF-β1 is important for maintaining c-myc$^+$ BCCs in cocultures, it cannot supplement PPT-I in the formation of cocultures (Fig. 9, *open circles*). The results also show that in the absence of c-myc, factors other than TGF-β have predominant roles as mediators of BCC growth in coculture.

DISCUSSION

This study reports on the analyses of the mechanisms by which PPT-I is involved in BCC integration among BM stroma (7). The studies used a previously reported coculture model of BM stroma and BCCs (7). Because the model represents an early period of BCC entry in the BM and the studies were verified with cells from primary BC, the findings provide insights in early cancer invasion of BM. The

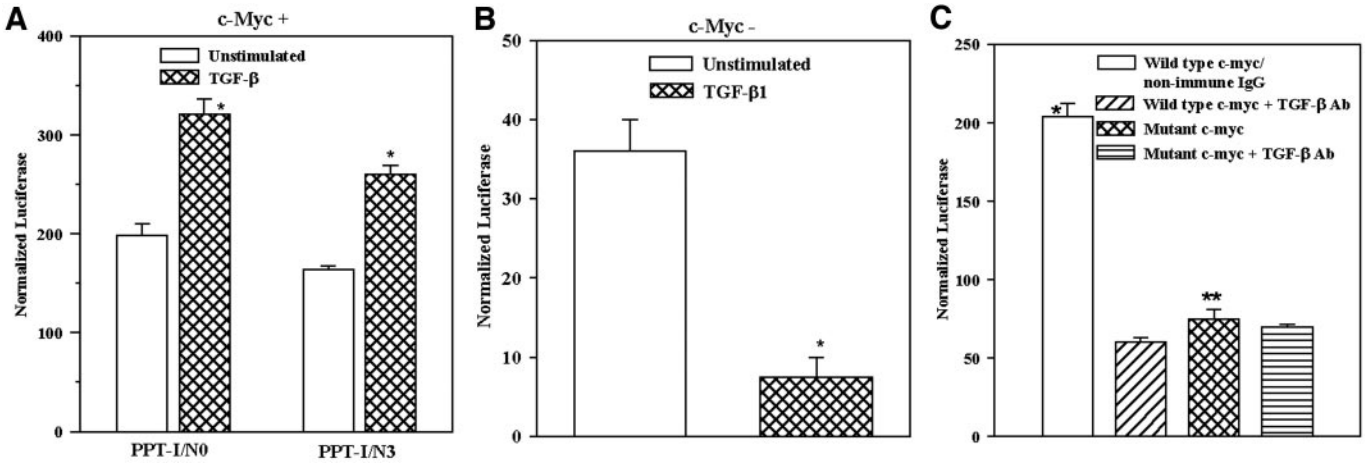

Fig. 8. Effects of endogenous and exogenous TGF-β on c-myc-mediated induction of PPT-I. *A*, BCCs (three cell lines and three primary cells, c-myc$^+$) were transfected with PPT-I/N0 (c-myc, *sites a* and *b*) or PPT-I/N3 (c-myc, *site b*). After 24 hours, cultures were stimulated with 10 ng/ml TGF-β1 for 10 hours. Normalized luciferase activities are presented as the mean ± SD, $n = 6$. *, $P < 0.05$ *versus* unstimulated cultures. *B*, effects of TGF-β on c-myc$^-$ cells. Non-tumorigenic breast cells were determined to be negative for c-myc by Western blots (not shown). Cells were transfected with pGL3-PPT-1/N0 and then stimulated with 10 ng/ml TGF-β1. The results are the mean ± SD, $n = 15$ for five different cell lines, each assayed in three different experiments. *, $P < 0.05$ *versus* unstimulated transfectants. *C*, pGL3-PPT-I/N0 (with wild-type or double-mutant c-myc sites) was transfected in c-myc$^+$ BCCs. Cultures contained 2 ng/ml anti-TGF-β or equivalent non-immune rabbit IgG. At 48 hours of transfection, luciferase activities were determined and then normalized with β-gal. The results are the mean ± SD, $n = 18$ for three BC cell lines and three primary BCCs, each tested in three different experiments. *, $P < 0.05$ *versus* the other experimental points; **, $P > 0.05$ *versus* mutant c-myc with anti-TGF-β.

model is particularly useful because it could circumvent some of the inherent problems associated with studies on cancer metastasis in mice, which rarely formed cancer.

Use of cytokine and transcription factor microarrays provides clues on the molecular relationship among TGF-β, c-myc, and PPT-I to facilitate BCC integration within BM stroma (7). Cytokine production in BCC and BM stroma after cocultures (Figs. 5 and 6) is consistent with the complex biology between PPT-I and cytokines, suggesting that future studies will need to dissect the pathways between PPT-I peptides and cytokines in the early integration of BCCs as part of the BM microenvironment (24). TGF-β was demonstrated to be a relevant facilitator in PPT-I-mediated integration of BCCs among stromal cells (Figs. 9*A* and *B*, *solid squares*). Despite the relevance of TGF-β, it is not an alternate for PPT-I (Figs. 9*A* and *B*, *open circle*). We observed the formation of cocultures, regardless of c-myc status (7; Figs. 9*A* and *B*). This suggests that TGF-β might be regulating the PPT-I gene via signaling pathways that do not involve c-myc. This is not surprising considering that cAMP-responsive element-binding proteins (CREBs) have been shown to be relevant to the induction of PPT-I (19).

An explanation for TGF-β1 as a negative regulator of luciferase activity in c-myc$^-$ BCCs (Fig. 8*B*) could be explained by the formu-

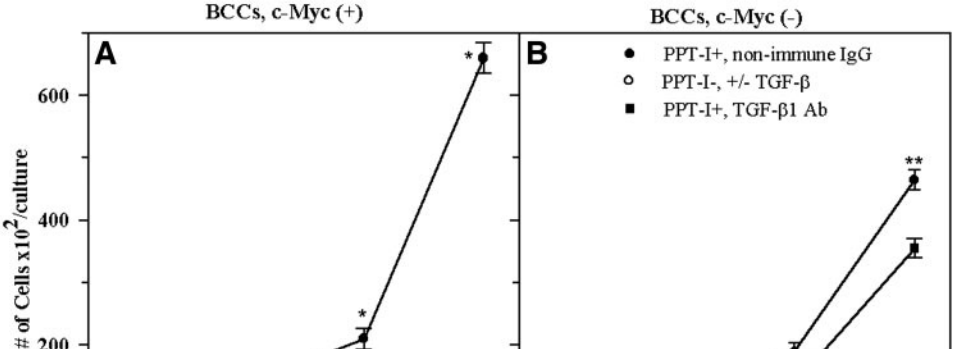

Fig. 9. Role of TGF-β in the integration of BCCs within BM stroma. BCCs (four cell lines and four primary cells), c-myc$^+$ (*A*) or c-myc$^-$ (*B*) were cocultured with BM stroma. Cultures contained TGF-β1 neutralization Ab, equivalent amounts of non-immune rabbit IgG, or untreated. Similar cultures were performed with PPT-I-BCCs, in the presence or absence of different amounts of exogenous TGF-β1. At different times during culture, the total numbers of cytokeratin-positive cells were counted. The results are presented as the mean ± SD, $n = 8$ for four BC cell lines and four primary BCCs. The levels of TGF-β and substance P in cocultures were quantitated, mean ± $n = 8$ (*C*). *, $P < 0.05$ *versus* similar cultures with TGF-β Ab (■). **, $P < 005$ *versus* 4-week time point in cultures treated with TGF-β Ab (■). ‡, $P < 0.05$ *versus* equivalent cultures with non-immune IgG. ∫, $P > 0.05$ *versus* parallel cultures with non-immune IgG.

C

BCCs c-Myc Status	Treatment of Cocultures	Substance P (pg/ml)	TGF-β1 (pg/ml)
Positive	Non-immune IgG	450±28	35±3
Positive	TGF-β Ab	35±4	<5
Negative	Non-immune IgG	320±19	42±4
Negative	TGF-β Ab	297±15	<5

lation of a hypothesis based on the effects of TGF-β1 on PPT-I induction in normal BM stroma. TGF-β-stimulated stroma showed reduced levels of PPT-I mRNA and its major peptide, substance P, compared with IL-1α (Fig. 2*C*). The blunted expression of PPT-I by TGF-β1 in stroma is consistent with the negative and positive hematopoietic effects of TGF-β1 and substance P, respectively (24, 26). Thus if TGF-β is required to negatively regulate hematopoiesis, it should not induce the expression of PPT-I. It has been hypothesized that TGF-β exerts cell cycle check through the repression of c-myc in normal cells (29). This suggests that c-myc$^-$ BCCs might be responding as normal cells with respect to TGF-β stimulation and that other pathways other than those involving c-myc might be operative.

The evolutionary conserved nature of the PPT-I gene, combined with its ability to induce different cytokines justify the focus on the PPT-I and TGF-β genes as facilitators of BCC metastasis to the BM. PPT-I exerts pleiotrophic functions with regards to cytokine production (24). This suggests that in the event of constitutive production of PPT-I in BCCs during the time when there are relatively few mutations, PPT-I could induce many cytokines to facilitate invasion of BCCs in the BM.

The distribution of cytokines produced by the BCCs before and after cocultures supports that the coculture model might represent an early stage of BC in the BM, at a time before bone invasion. At this time, we cannot explain why platelet-derived growth factor is up-regulated in the cocultures (Fig. 5). Perhaps platelet-derived growth factor might be important to the maintenance of BM functions when BCCs are in the microenvironment. The impetus for this assumption is the common roles of substance P, the major PPT-I peptide, and platelet-derived growth factor in bone formation (6, 30). Two interesting findings are related to insulin-like growth factor and TGF-β production; insulin-like growth factor production was similar in BCCs before and after coculture (Fig. 5*A*) whereas TGF-β production was reduced (Fig. 6). Because insulin-like growth factor and TGF-β are both linked to bone resorption, it is tempting to propose that the profiles of these cytokines might be explained by their functions to maintain homeostasis in the BM microenvironment. This will be advantageous for the BCCs to survive and also to remain undetectable at a period before clinical detection.

Studies show that PPT-I is regulated differently in BCCs, compared with non-tumorigenic mammary epithelial cells (18, 19). In BCCs, PPT-I translation is enhanced by cytoplasmic factors (18). Ongoing studies using proteomics suggest that a protein of M_r equivalent to 15 kilodaltons might be involved in binding of the untranslated region of the PPT-I mRNA so as to increase in the rate of translation.[7] Together, these differences in PPT-I regulation might explain the significantly high activities in the 5′ flanking region of PPT-I in non-tumorigenic cells, compared with BCCs (Fig. 3).

TGF-β levels changed in both BCCs and stromal cells during different levels of cell confluence.[7] Perhaps there is a gradient dependency on TGF-β for EMST transition. TGF-β levels are significantly reduced in cocultures (Fig. 6). Because TGF-β has been shown to induce PPT-I-reporter gene activities (Fig. 8*A*), increased PPT-I mRNA and reduced levels of TGF-β in confluent coculture BCCs (Figs. 2*A* and *B* and 6) appear contradictory. Endogenous TGF-β appears to be important for PPT-I activities in BCCs (Fig. 8*C*). Perhaps TGF-β production in both stromal cells and BCCs might be involved in autocrine and/or paracrine activation of PPT-I in cocultures. TGF-β-c-myc-PPT-I axis, although relevant to the formation of cocultures by BCCs and BM stroma (Fig. 9*A*), is not the only mechanism by which BCC integrate as part of BM stroma. This is evident by minimal effects of TGF-β Ab in the growth of c-myc$^-$ BCCs in cocultures (Fig. 9*B*).

We reported previously that hematopoietic activities are not affected by the cocultures of BCCs and BM stroma (7). Studies with cytokine microarrays have provided insights on this observation (Fig. 5). The different groups of cytokines produced or down-regulated in cocultures might offset excessive stimulatory and inhibitory effects on hematopoiesis so as to maintain hematopoietic homeostasis. For example, increased TGF-β production in stroma and BCCs might be "offset" by the production of stimulatory cytokines such as stem cell factor (Figs. 5 and 6). Studies to determine how multiple cytokines are involved with PPT-I in BCC integration among stroma are ongoing experiments.

EMST, assigned as the method by which BCCs retain a quiescent phenotype among BM stroma (7), is probably mediated by TGF-β on BCCs that have already undergone epithelial to mesenchymal transition (25). The reason for implicating TGF-β in EMST is based on its role in autocrine reversion of epithelial to mesenchymal transition and its property as a mediator of "functional plasticity" in epithelial cells (31, 32). To understand the role of TGF-β is important because TGF-β/Smad signaling pathways are potential targets for cancer treatment (33).

The regulation of fragments within the 5′ flanking region of the PPT-I gene shows similar trends in breast and BM cells (Fig. 3). However, the activities of PPT-I/N0 were the highest in stroma (Fig. 4). This was surprising because subsequent studies show that the same inserts were increased in BCCs (Fig. 7*E*). The differences were explained by studies with c-myc$^+$ and c-myc$^-$ BCCs (Figs. 3 and 4), compared with Fig. 7*E* in which studies used only c-myc$^+$ BCCs.

Computer analyses of PPT-I/N0 for TF motifs showed consensus regions for multiple TF, suggesting that PPT-I could be influenced by BM microenvironmental factors. This report indicates that at least one c-myc site is sufficient for optimum activity of PPT-I in BCCs (Fig. 7*E*). The effects of TGF-β on PPT-I induction in BCCs is different for normal BM stroma in which TGF-β blunted the induction of PPT-I (Fig. 2*C*). Other cytokines could be involved in the activities of PPT-I because neutralization of endogenous TGF-β did not completely blunt the activity of PPT-I/N0 (Fig. 8*B*). Perhaps cytokines that induce CREB might be relevant, as reported previously for the regulation of PPT-1 (19) and as suggested in the microarray studies (Table 2). Because the PPT-I promoter has two binding sites for CREB (19), perhaps the presence of nuclear CREB in BCCs might explain why PPT-I/N0 with mutant c-myc sites were activated above baseline levels (vector alone; Fig. 8*C*). *MYC* overexpression has been shown to disrupt the repair of double-stranded DNA breaks (34), suggesting that PPT-I might be indirectly involved in DNA damage of BCCs. The role of c-myc in PPT-I being able to protect cancer cells from undergoing apoptosis is yet to be studied (35). The link between TGF-β and PPT-I expands on other reports on bone biology where TGF-β is linked to other genes such as IL-11 (36).

Microarray analyses show that PPT-1 induces different cytokines and chemokines, which could be involved in cell cycle progression (Fig. 5). Despite the controversies within the major research groups regarding the genes and uniqueness of cancer cells that metastasize to the BM (10), there is no doubt that cancer metastasis to the BM leads to poor prognosis (8). Interestingly, preference for the BM is common for cancers with the highest frequencies: breast, lung, prostate, and to a lesser extent colon. This report contributes to BM metastasis of cancer through studies that demonstrate a role for PPT-I and also show that this gene could be subjected to microenvironmental influence in the BM (*i.e.* stromal cells). Undoubtedly, an understanding of intercellular interactions between cancer cells and resident BM cells during the early period of cancer development would aid in the early

[7] D. Cinco, F. Caputo, R. Murthy, P. Rameshwar, unpublished data.

detection of cancer in the BM and perhaps prevent further invasion to the BM.

REFERENCES

1. Wulf GG, Jurgens B, Liersch T, et al. Reverse transcriptase/polymerase chain reaction analysis of parathyroid hormone-related protein for the detection of tumor cell dissemination in the peripheral blood and bone marrow of patients with breast cancer. J Cancer Res Clin Oncol 1997;123:514–21.
2. Mullersieburg CE, Deryugina E. The stromal cells' guide to the stem cell universe. Stem Cells 1995;13:477–86.
3. Moore KA, Ema H, Lemischka IR. In vitro maintenance of highly purified, transplantable hematopoietic stem cells. Blood 1997;89:4337–47.
4. Taback B, Giuliano AE, Hansen NM, Singer FR, Shu S, Hoon DSB. Detection of tumor-specific genetic alterations in bone marrow from early-stage breast cancer patients. Cancer Res 2003;63:1884–7.
5. Mansi JL, Berger U, McDonnell T, et al. The fate of bone marrow micrometastases in patients with primary breast cancer. J Clin Oncol 1989;7:445–9.
6. Mundy GR. Metastasis to bone: Causes, consequences and therapeutic opportunities. Nature Rev 2002;2:584–92.
7. Rao G, Patel PS, Idler SP, et al. Facilitating role of preprotachykinin-I gene in the integration of breast cancer cells within the stromal compartment of the bone marrow: a model of early cancer progression. Cancer Res 2004;64:2874–81.
8. Braun S, Pantel K, Muller P, et al. Cytokeratin-positive cells in the bone marrow and survival of patients with stage I, II, or III breast cancer. N Eng J Med 2000;342:525–33.
9. Kittler-Schmidt O, Ragg T, Daskalakis A, et al. From latent disseminated cells to overt metastasis: genetic analysis of systemic breast cancer progression. Proc Natl Acad Sci USA 2003;100:7737–42.
10. Couzin J. Tracing the steps of metastasis, cancer's menacing ballet. Science (Wash D C) 2003;299:1002–6.
11. Guttmacher AE, Collins FS. Breast and ovarian cancer. New Engl J Med 2003;348:2339–47.
12. Whittemore AS, Gong G, Intnyre J. Prevalence and contribution of BRCA1 mutations in breast cancer and ovarian cancer: results from three U.S. population-based case control studies of ovarian cancer. Am J Hum Genet 1997;60:496–504.
13. Moharita A, Harrison JS, Rameshwar P. Neurokinin receptors and subtypes as potential targets for breast cancer: relevance to bone marrow metastasis. Drug Design Reviews Online. In press, 2004.
14. Rameshwar P, Oh HS, Yook C, Gascon P, Chang VT. Substance P-Fibronectin-Cytokine interactions in myeloproliferative disorder with bone marrow fibrosis. Acta Haematologica 2003;109:1–10.
15. Pennefather JN, Lecci A, Candenas ML, Patak E, Pinto FM, Maggi CA. Tachykinins and tachykinin receptors: a growing family. Life Sci 2004;74:1445–563.
16. Rameshwar P, Poddar A, Gascon P. Hematopoietic regulation mediated by interactions among the neurokinins and cytokines. Leuk Lymphoma 1997;28:1–10.
17. Bandari PS, Qian J, Oh HS, et al. Crosstalk between neurokinin receptors is relevant to hematopoietic regulation: cloning and characterization of neurokinin-2 promoter. J Neuroimmunol 2003;138:65–75.
18. Singh D, Joshi DD, Hameed M, et al. Increased expression of preprotachykinin-I and neurokinin receptors in human breast cancer cells. Implications for bone marrow metastasis. Proc Natl Acad Sci USA 2000;97:388–93.
19. Qian J, Yehia G, Molina C, et al. Cloning of human preprotachykinin-I promoter and the role of cyclic adenosine 5′-monophosphate response elements in its expression by IL-1 and stem cell factor. J Immunol 2001;166:2553–61.
20. Amati B. Integrating Myc and TGF-β signaling in cell-cycle control. Nature Cell Biol 2001;3:E112–3.
21. Kretzschmar M. Transforming growth factor-β and breast cancer: transforming growth factor-β/SMAD signaling defects and cancer. Breast Cancer Res 2000;2:107–15.
22. Joshi DD, Dang A, Yadav P, et al. Negative feedback on the effects of stem cell factor on hematopoiesis is partly mediated through neutral endopeptidase activity on substance P: a combined functional and proteomic study. Blood 2001;98:2697–706.
23. Rameshwar P, Narayanan R, Qian J, Denny TN, Colon C, Gascón P. NF-κB as a central mediator in the induction of TGF-β in monocytes from patients with idiopathic myelofibrosis: an inflammatory response beyond the realm of homeostasis. J Immunol 2000;165:2271–7.
24. Rameshwar P. Substance P: a regulatory neuropeptide for hematopoiesis and immune functions Clin Immunol Immunopath 1997;85:129–33.
25. Massague J, Chen YG. Controlling TGF-β signaling. Genes Dev 2000;14:627–44.
26. Janowska-Wieczorek A, Majka M, Ratajczak J, Ratajczak MZ. Autocrine/paracrine mechanisms in human hematopoiesis. Stem Cells 2001;19:99–107.
27. Wakefield LM, Roberts AB. The two faces of transforming growth factor β in carcinogenesis. Proc Natl Acad Sci USA 2003;100:8621–3.
28. Kim SJ, Leterio J. Transforming growth factor-β signaling in normal and malignant hematopoiesis. Leukemia 2003;17:1731–7.
29. Alexandrow MG, Moses HL. Transforming growth factor-β and cell cycle regulation. Cancer Res 1995;55:1452–7.
30. Rameshwar P, Poddar A, Zhu G, Gascón P. Receptor induction regulates the synergistic effects of substance P with IL-1 and PDGF on the proliferation of bone marrow fibroblasts. J Immunol 1997;158:3417–24.
31. Zeisberg M, Hanai J, Sugimoto H, et al. BMP-7 counteracts TGF-β1-induced epithelial-to-mesenchymal transition and reverses chronic renal injury. Nat Med 2003;9:964–8.
32. Zavadil J, Bitzer M, Liang D, et al. Genetic programs of epithelial cell plasticity directed by transforming growth factor-β. Proc Natl Acad Sci USA 2001;98:6686–91.
33. Suh N, Roberts AB, Reffey SB, et al. Synthetic triterpenoids enhance transforming growth factor β/Smad signaling. Cancer Res 2003;63:1371–6.
34. Karlsson A, Deb-Basu D, Cherry A, Turner S, Ford J, Felshner DW. Defective double-strand DNA break repair and chromosomal translocations my MYC overexpression. Proc Natl Acad Sci USA 2003;100:9974–9.
35. Reeve JG, Bleehem NM. [D-ARG[1], D-PHE[5], D-TRP[7,9], LEU[11]] substance P induces apoptosis in lung cancer cell lines in vitro Biochem Biophys Res Commun 1994;199:1313–9.
36. Kang Y, Siegel PM, Shu W, et al. A multigenic program mediating breast cancer metastasis to bone. Cancer Cell 2003;3:537–49.